Journal of Nepal Geological Society, 2020, vol. 60, pp. 21-36
https://doi.org/10.3126/jngs.v60i0.31257

Contribution of fault geometry to probabilistic seismic hazard in intermontane basin: An example from Kathmandu Valley

Govinda Prasad Niroula[1] and *Deepak Chamlagain[2]

[1]Kathford International College of Engineering and Management, Tribhuvan University, Lalitpur, Nepal
[2]Department of Geology, Tri-Chandra Multiple Campus, Tribhuvan University, Kathmandu, Nepal
[*]Corresponding author's email: deepakchamlagain73@gmail.com

ABSTRACT

The intermontane basins of the Himalaya are prone to damaging earthquakes as they are located roughly 10-15 km above the Main Himalayan Thrust (MHT), a major seismogenic thrust fault in the Himalaya. After the Mw 7.8 2015 Gorkha earthquake, the geometry of the MHT has been investigated using different approaches. Two contrasting models with a single ramp and double ramp geometries are proposed. However, the contribution of these geometries on seismic hazard has not been investigated yet. In this contribution, therefore, a probabilistic seismic hazard assessment is carried out using both models for Kathmandu valley and the obtained results are compared with the measured strong ground motion data of main shock of the 2015 Gorkha seismic sequence at Kirtipur, Kathmandu (rock site). It is found that the areal sources have the least contribution indicating sole contribution of MHT to relatively higher level of seismic hazard in the valley located on the up-dip locked portion of the MHT. The Peak Ground Acceleration (PGA) of the main shock of the 2015 Gorkha earthquake and PGA for 760 yr (exposure period of 50 yr and probability of exceedance 6.36%) of return period adopting both single and double ramp models are approximately same with error level of ± 3.84%. The results indicate that the adopted seismic model fairly represents the seismo-tectonic of the region, particularly of the MHT. Considering this as the best fit results, the spatial distribution of the seismic hazard is analysed using double ramp model. It is found that the PGA values in the valley for 760 yr return period vary from 0.24 g to 0.28 g. The PGA values are higher in the southern part and gradually decrease towards north. Such decrease in PGA is consistent with the decrease in locking level of the MHT towards north. The study, therefore, emphasizes detailed geometrical characterization of the MHT while carrying out the seismic hazard assessment in the Himalaya.

Key words: Main Himalayan Thrust; Seismic hazard; 2015 Gorkha earthquake; Kathmandu valley

Received: 4 June, 2020 **Received in revised form:** 27 August, 2020 **Accepted:** 28 August, 2020

INTRODUCTION

The intermontane basins of the Himalaya are prone to earthquake shaking as they are located 5 km to 10 km above the seismogenic thrust fault. Kathmandu valley is one of the intermontane basins that witnessed several devastating earthquakes in the past, e.g. earthquake of 1255, 1404, 1681, 1803, 1810, 1833, 1866, 1934, 1985, 2015 etc. (Pant, 2002; Avouac et al., 2015). The earthquake of 1255 AD killed about one-third population of the valley including the then King Abhaya Malla, who was severely injured by the event. Since then, the earthquake of 1833 also caused massive damage in the valley. The great earthquake of 1934, which had epicentre in eastern Nepal, hit Kathmandu valley terribly. The earthquake killed 8519 people in Nepal only out of which Kathmandu valley accounted for 4296 deaths. Beside human loss, physical destruction was massive, about two-hundred thousand houses were damaged in different scales. In Kathmandu valley alone, 55,739 houses were damaged at different scales out of which 12,397 were completely destroyed (Rana, 1935). After eighty years of the great earthquake of 1934, Kathmandu valley suffered a huge loss of human and physical infrastructures during the Mw 7.8 2015 Gorkha earthquake. A total of 8970 people lost their lives out of which 1750 were from Kathmandu valley (MoHA, 2016). These data base have reflected the inherited seismic hazard and risk in Kathmandu valley.

Seismic source characterization is one of the key steps in seismic hazard assessment in the valley like Kathmandu that lies above the seismogenic fault. The contribution of seismic sources, either aerial or fault, to the assessment of seismic hazard is primarily based on how the sources are characterized. It is crucial to investigate relative contribution of various fault geometries to seismic hazard level. In case of Nepal Himalaya, few studies have been carried out

to quantify the seismic hazard (e.g. Thapa and Wang, 2013; Rahman et al., 2017; Stevens et al., 2018). Both aerial and fault sources are considered in terms of length of segment but their relative contribution to seismic hazard assessment incorporating geometry has not been considered yet (e.g. Thapa and Wang, 2013; Rahman et al., 2017). Stevens et al. (2018) computed seismic hazard for Nepal considering both aerial and fault sources, however, variation of geometry of the MHT has not been considered to estimate its relative contribution to hazard estimation. Because of location of intermontane basin like Kathmandu valley just above the complex seismogenic MHT, the seismic hazard and risk is expected to be high. In this contribution, therefore, it is aimed to assess the seismic hazard probabilistically for Kathmandu valley considering both aerial and fault sources with different geometries of the MHT. The results are then compared with the strong ground motion of the 2015 Gorkha earthquake measured at the rock site of Kirtipur, southern part of Kathmandu valley. The reason behind this comparison is an inter-seismic period between two successive devastating earthquakes, i.e. the 2015 Gorkha and 1255 earthquakes that occurred in central Nepal. After 760 years, the 2015 Gorkha earthquake ruptured the MHT beneath the Kathmandu valley but did not reach to the surface. This segment of the MHT was also ruptured by the 1255 earthquake and reached up to the MFT (Wesnousky et al., 2017a). Taking inter-seismic period of 760 yr as a return period in probabilistic seismic hazard calculation, the PGA is compared with that of the 2015 Gorkha earthquake (main shock).

GEO-TECTONICS OF KATHMANDU REGION

Geo-tectonically, Kathmandu valley is located in lesser Himalayan region of central Nepal. It lies on the large crystalline thrust sheet, the Kathmandu Nappe, which consists of low to medium grade metamorphic rocks and overlying fossiliferous sedimentary sequence of Tethyan sediments (Stöcklin and Bhattarai, 1977) (Fig. 1). The structural data have revealed a bowl shaped basin with varying depths and isolated scattered bedrock hillocks in the valley. Moribayashi and Maruo (1980) investigated basement topography of the valley by gravity survey. Using two-layer model, i.e. Quaternary sediments and the underlying Paleozoic basement meta-sediments, the interface was identified based on the observed density difference of 0.8 g/cm$^{3.}$ Geologically, the valley is divided into two parts; the northern part of the valley is dominated by sandy facies sediments and southern half is mostly comprises of black clay deposits (Sakai, 2001). Based on gravity data, the maximum depth to the basement is estimated to be about 650 m (Moribayashi and Maruo, 1980). Beside this, number of boreholes were driven in the past to explore the subsurface geology of the valley, which have revealed more than 300 m thick clayey and sandy sediments (Katel et al., 1996).

Thrust system

The Himalaya is characterised by a fold-and-thrust belt that comprises of three major south verging thrust system, namely Main Frontal Thrust (MFT), Main Boundary Thrust (MBT) and Main Central Thrust (MCT) from south to north (Le Fort, 1975) (Fig. 1). The MFT is the boundary thrust between the Indo-Gangetic plain that comprises of recent alluvial deposits of the Himalayan Rivers and the Siwalik, which comprises of thick sedimentary sequence of mudstone, sandstone and conglomerate from bottom to top. The MBT separates the underlying Siwalik with overlying Lesser Himalayan Sequence that consists mostly of low-grade metamorphic, occasionally meta-sedimentary rocks. The MCT is located in-between the underlying Lesser Himalayan Sequence and overlying Higher Himalayan Sequence consisting of high-grade metamorphic rocks, e.g. kyanite-sillimanite gnesiss, schist and quartzite. Beside these thrusts, a detachment

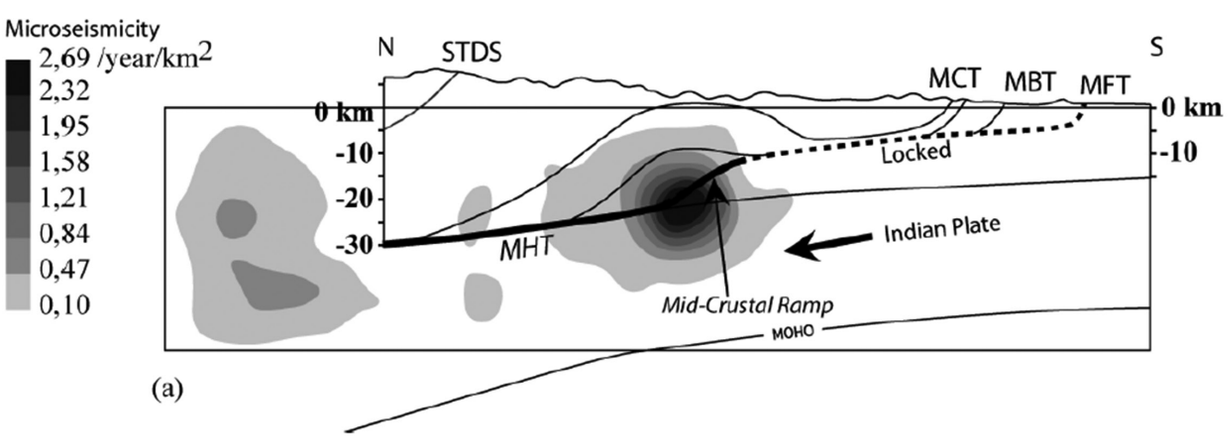

Fig. 1: North-South geological cross-section of Nepal Himalaya showing major thrust system and micro-seismicity (Pandey et al., 1999). MFT: Main Frontal Thrust; MBT: Main Boundary Thrust; MCT: Main Central Thrust; STDS: South Tibetan Detachment System.

system of normal faults is present above the Higher Himalayan Sequence to separate the overlying thick sedimentary sequence of Tibetan Tethys Himalaya in the northern most part of the Himalayan range reflecting the inversion tectonics. These all thrust faults are the splay faults of the basal Main Himalayan Thrust (MHT) that is exposed as a MFT in the frontal part of the Siwalik.

Main Himalayan Thrust (MHT)

Main Himalayan Thrust (MHT) is a key plate boundary thrust between the Indian and Eurasian plates that governs the structure, tectonic and seismicity of the Himalayan belt (Fig. 1). The convergence of the Indian Plate along the MHT is about 2 cm/yr that significantly contribute to strain accumulation in central Nepal Himalaya (Ader et al., 2012). The structural, geophysical, seismic and geodetic model have revealed a mid-crustal ramp along the MHT that coincides the topographical break at the frontal part of the Higher Himalaya (Schelling and Arita, 1991; Decelles et al., 2001; Ader, et al., 2012). The ramp structure is probably located at 15 km depth in the central Nepal and varies laterally. After the 2015 Gorkha earthquake, several studies have been carried out on geometry of the MHT (e.g. Elliot et al. 2016; Hubbard et al., 2016; Wang et al., 2017). These studies along with the earlier have come up with two contrasting models; the single and double ramp along the MHT. The single ramp model in eastern Nepal basically relies on structural data from which geometry was inferred (Schelling and Arita, 1991). The magnetotelluric data in the central Nepal has revealed a highly conductive zone in the Higher Himalayan front that resembles with mid-crustal ramp shown by structural model (Lemonnier et al., 1999). Elliot et al. (2016), using geodetic data combined with geologic, geomorphological and geophysical data, came up with a steep thrust fault flattening at depth of 5 to 15 km that connects the single mid-crustal ramp with steeper thrust. The estimated dip of southern and northern flat is about 7^{o} and 5^{o} -7^{o} respectively with 20^{o} dip of the mid-crustal ramp. In contrast, Hubbard et al. (2016) proposed a double ramp model by comparing structural model with the slip inversion data of the 2015 Gorkha earthquake; the moderate ramp is inferred at depth of 10 km and deep ramp is at 15 km depth with dip angle of 26^{o}. The dip of the southern flat is in-between 2^{o}-5^{o}, middle flat and northern flat is 7^{o}. Further, a double ramp model was also proposed based on the horizontal location of the 2015 Gorkha seismic sequence (Wang et al., 2017). The dip of flat portion the MHT was found to be 7o towards north and both ramps have steep dip, i.e. 26o. These new information on geometry of MHT is important to understand their contribution to seismic hazard in the region.

SEISMICITY

The seismicity in Nepal Himalaya is mainly governed by movement along the MHT. The ramp structure along the MHT is the main geometrical asperity, though single or double, that constantly accumulates elastic strain during the inter-seismic period (Pandey et al., 1995 and 1999). The intermittent release of such elastic strain causes micro- to small tremors. The significant release of the accumulated strain generates the great earthquakes often causing rupture along the MFT. The deep ramp structure is located just beneath the Higher Himalayan front along the strike of the Himalaya, which is characterised by intense seismicity (Pandey et al., 1995).

The record of historical seismicity in the region is scrubby. Most of the records are from chronicles and limited paleoseismological studies. The major events in Nepal that caused significant damages in Kathmandu valley were of 1255, 1344, 1408, 1681, 1803, 1833, 1866 and 1934 earthquakes. These earthquakes were originated due to rupture along the MHT, some of them ruptured the up-dip section of the MHT and reached up to the surface, i.e. MFT. Clusters of instrumental seismicity are seen in eastern, central (north of Kathmandu valley) and western Nepal (Fig. 2). The projection of these events are clustered in and around the ramp structure of the MHT (Pandey et al., 1995 and 1999; Wang et al., 2017) (Fig. 1).

The Mw 7.8 Gorkha Earthquake

On 25th April, 2015 at 11:56 AM, an earthquake of magnitude 7.8 occurred at Barpak village of Gorkha district and jolted central Nepal (Avouac et al., 2015). The tremor of the earthquake was felt beyond the Nepalese territory, i.e. Delhi in south, Bhutan in the east, NW Indian territory in the west and south Tibet of China to the north. The earthquake was thrust fault type and unzipped the locked hinge of the mid-crustal ramp along the MHT at the depth of 15 km and the rupture propagated about 140 km from Barpak to Dolakha and arrested at the strain shadow zone of 1934 earthquake slip areas (Avouac et al., 2015). The strong ground motions of the main shock were recorded during the earthquake at the KTP site, and other sites in the basins. The Peak Ground Accelerations (PGAs) were relatively small at the both KTP and basin sites (Takai et al. 2016). The measured PGA at KTP is 0.24 g, 0.15 g and 0.12 g for EW, NS and UD components. Dhakal et al. (2016) attributed the strong long-period motions in the basin to the amplification effect of low velocity sediments

in the basin. The horizontal components of strong ground motion were de-convolved using measured shear wave velocity, shear modulus, damping ratio and unit weight (Table 1 and Fig. 3). The square root of sum of square (SRSS) for de-convolved horizontal PGAs for the main shock event was 0.26 g. This value is used as a reference value to compare with computed PGA at Kirtipur.

Table 1: Adopted parameters for deconvolution of measured acceleration time history at KTP rock site.

Layer no	Thick-ness (m)	Shear wave velocity (V_S, m/s)	Unit weight (kN/ m^3)	Soil proper-ties
1	1	230	18	PI30
2	1	235	18	PI30
3	9	367	19	PI30
4	1	406	19	PI30
5	2	418	20	PI30
6	1	598	20	PI15
7	2	899	21	PI15
8	2	1339	21	PI15
9	1	1524	21	PI15
10	-	2506	22	Rock

PROBABILISTIC SEISMIC HAZARD ASSESSMENT (PSHA)

Cornell (1968) developed a methodology for PSHA and is used to provide a framework in which uncertainties in size, location and rate of recurrence of earthquakes can be considered to provide a probabilistic understanding of seismic hazard. In addition, to minimize the uncertainty of earthquake source parameters, a logic tree is implemented in this study. The following sections provide steps of probabilistic hazard computation.

Earthquake catalogue

Earthquake catalogue is fundamental to provide key basis for seismic source characterization. The distribution of the earthquake events are mainly governed by the seismo-tectonics of the particular site. The uniformly distributed seismicity within the similar tectonic environment greatly contributes for assessing the key seismicity parameters including the mean seismic activity, the *b* value of the frequency–magnitude Gutenberg–Richter relation, and the maximum expected earthquake magnitude of the study area.

Nepal has only started earthquake monitoring by its networks since 1994 as a result it has very short archive of the earthquake events measured by 21

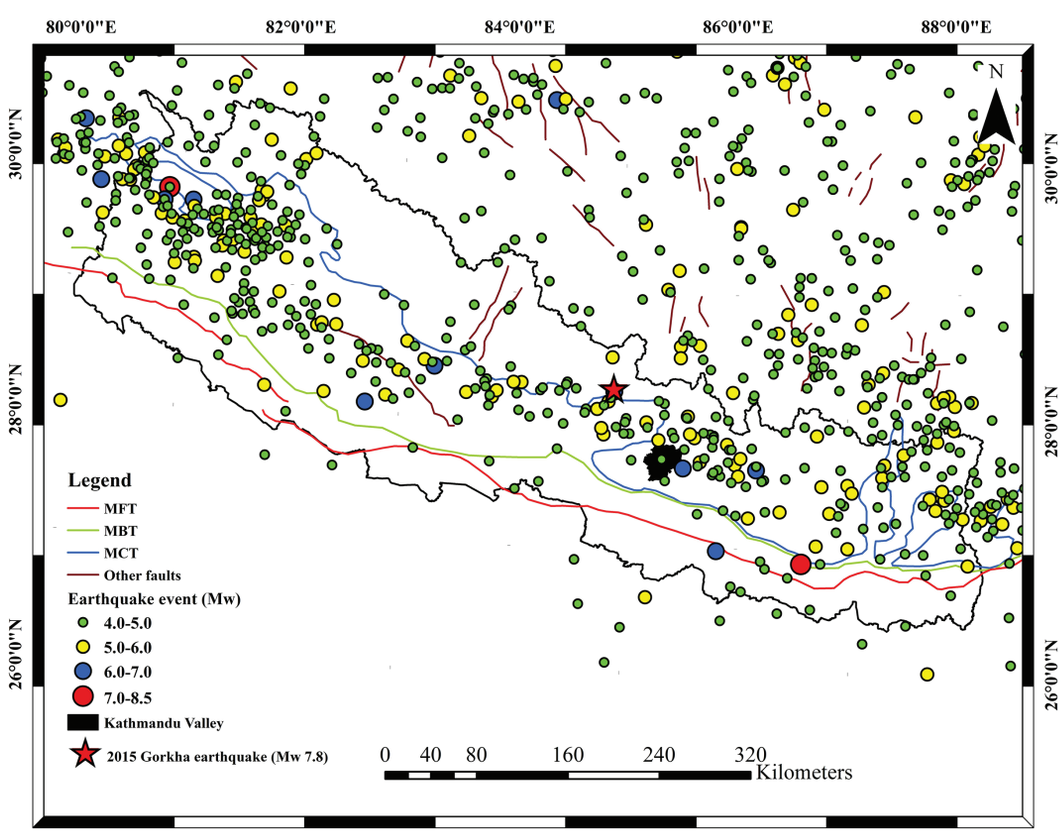

Fig. 2: Declustered seismicity of Nepal and adjacent areas (Data source: International Seismological Centre).

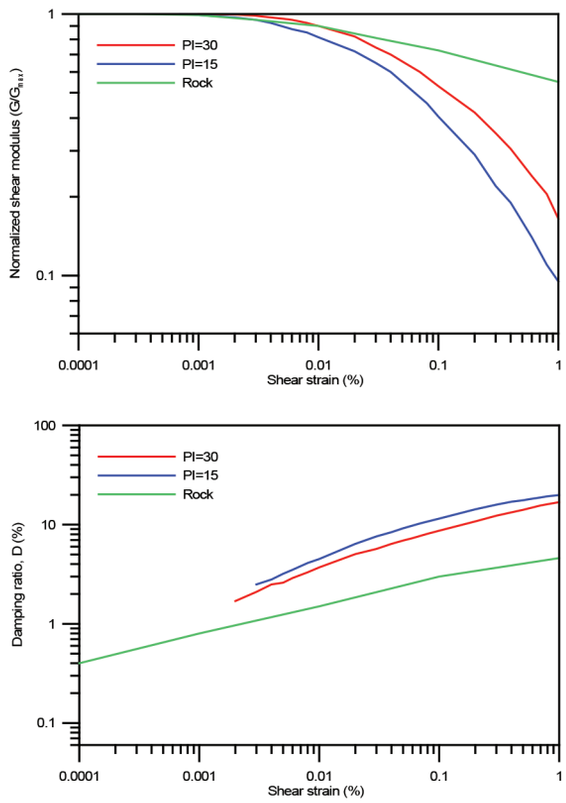

Fig. 3: Material properties used for deconvolution of horizontal acceleration time histories of main shock of 2015 Gorkha earthquake. The soil curve for Plasticity Index (PI) 15 and 30 are adopted from Vucetic and Dobry (1991) and for rock Schnabel (1973).

single component stations (Department of Mines and Geology, Nepal). In this study, therefore, earthquake catalogue of International Seismological Centre is used (ISC, http://www.isc.ac.uk/) (Fig. 2). ISC catalogue incorporates data from different monitoring networks, e.g. USGS, IRIS and many other national networks. This catalogue is complemented with the historical data archived from chronicles and paleoseimological studies throughout the Himalayas and around since 1100 AD. The catalogue is for the period between 1100 AD to April, 2019 AD. The historical earthquakes were considered for the assessment though their location are not well known. Declustering of the catalogue was done using the method given by Gardner and Knopoff (1974). Since the adopted catalogue consists earthquake events of different magnitude scales, all events were converted to the moment magnitude using the following equations given by Scordillis (2006).

$$Mw = 0.67Ms + 2.07\ (Ms \leq 6.1)$$
$$Mw = 0.99Ms + 0.08\ (Ms > 6.1)$$
$$Mw = 0.85mb + 1.03\ (mb \leq 6)$$
$$Mw = 1.69mb - 4.01(mb > 6)$$

Source Characterization

The tectonics of the Himalaya and adjacent region is complex. The Himalayan belt is characterised by the compressional tectonics, whereas the deformation pattern in the southern Tibet is mostly extensional as reflected by several graben structures and associated normal faults. Source characterization is difficult in case of Nepal Himalaya because of short archive of seismic events. Previous studies have considered different approaches to characterise the seismic source (e.g. Pandey et al., 2002; Thapa and Wang, 2011; Rahman et al., 2018). These studies were primarily based on linear and aerial sources avoiding the seismogenic MHT with its complex geometry. Based on these facts, seismic source delineation and characterization is carefully done by analysing the occurrence of large earthquakes, planar distribution of all earthquakes above certain level of magnitude, activity of seismogenic fault, shape of isoseismals, intensity distribution, neotectonic activity and regional tectonic framework. The source zones are divided into two broad categories; continental collision source and aerial sources. The seismic sources are described briefly below.

Continental Collision Source

The major intra-crustal thrust faults, namely MFT, MBT and MCT, are merged in a single low-angle major thrust fault MHT. Seismically, the crustal-scale thrusts faults MBT and MCT are not active at present-day neotectonic deformation rather MHT is active as it is the key structure for present-day convergence of the Indian Plate beneath the Eurasian Plate. Therefore, only the MHT is considered as a seismic source.

The MHT is a flat-ramp-flat geometry, where the northern flat is creeping, the southern flat is locked and the ramp itself is a transition zone that can be considered as the geometrical asperity to accumulate the elastic strain in the Himalayan seismic belt. The general dip of the MHT is very shallow, typically less than 10° with the flats dipping approximately 2° to 7° (Ader et al., 2012, Hubbard et al., 2016, Elliot et al., 2016). The thrust ramp geometry of the MHT produces three primary types of Himalayan earthquakes:

a) Moderate and micro earthquakes that occur within the vicinity of the ramp (clustered around the MHT ramp) at the transition from fault creep at depth to stick slip behavior towards the ground surface;

b) Large blind earthquakes (1805, 1833, possibly 1905, 2015) that rupture from the top of the ramp toward the MFT, but don't extend to the surface; and

c) Great earthquakes (1505, ~1400, 1255, possibly 1100) that extend to the surface, and likely down the ramp.

The largest thrust earthquakes along the Himalayan arc are associated with rupture lengths of similar scale (>400 km) to the largest of those that have occurred historically along the interface subduction zones (Lave et al., 2005; Mugnier et al., 2013; Wesnousky et al., 2017a, 2017b). Characteristics of the MHT have also led researchers to model the MHT in a similar manner as a subduction zone megathrust (Avouac et al., 2015; Kubo et al., 2016; Stevens et al., 2018). The historical as well as instrumental seismicity patterns and their characteristics in Nepal support the probability of very large (Mw > 9) earthquake in Nepal along this structure (Stevens and Avouac, 2016). Therefore, seismic sources associated with the activity along the MHT are modeled using characteristics similar to a subduction interface. To examine the contribution of MHT geometry, both single and double ramp structures are incorporated in the model. The adopted geometrical parameters are shown in Table 2. For a single ramp model (SRM), a geometry proposed by Elliot et al. (2016) was adopted, whereas for double ramp model (DRM), geometry proposed by Hubbard et al. (2017) was implemented. In the model, the MHT fault with both geometries is divided into several triangular elements for the computational purpose (Fig. 4). The other faults (MBT and MCT) are not considered for hazard estimation as the MBT is located in the locked segment of MHT and the MCT is seismically not active for a long time.

Table 2: Geometrical features of the Main Himalayan Thrust (MHT) for hazard estimation.

Outcropping (MFT)	Single Ramp Model (Elliot et al., 2016)				
	Southern Flat	Ramp		Northern Flat	
30°/ 10 km	7°/75 km	20°/30 km		7°/40 km	
	Double Ramp Model (Hubbard et al., 2016)				
21°/10 km	Southern Flat	Moderate Ramp	Middle Flat	Deep Ramp	Northern Flat
	5°/37 km	26°/8 km	7°/31 km	26°/30 km	7°/40 km

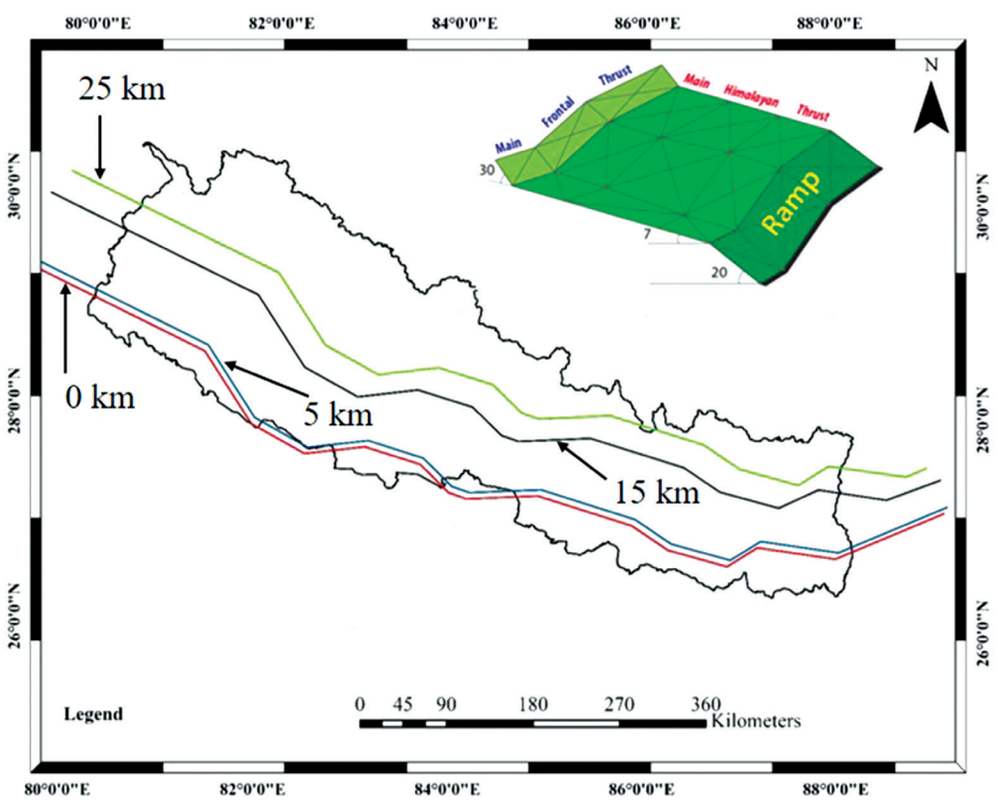

Fig. 4: Geometry of MHT (subduction interface) considered for the source characterization. The locked portion of the MHT plane is divided into several triangular elements for computation purpose. The 0, 5, 15, and 25 km show the depth to the MHT. The double ramp geometry is also incorporated in the same way considering the dimension shown in Table 2.

Areal Sources

Beside the fault source, the random or background earthquakes associated with other geological structures are considered in the PSHA by considering areal sources. Altogether six aerial sources are considered, which are represented by active shallow crust and stable continental area (Fig. 5).

Graben Source

Three sources are associated with the northern grabens in Tibet, e.g. North Graben-1, North Graben-2 and North Graben-3. Grabens of southern Tibet and the Himalaya represent the Cenozoic extensional tectonic phase, which had affected the whole Tibet and northernmost part of the Himalaya. These grabens are mainly distributed along the crest of the Himalaya, southern Tibet and central Tibet. The major grabens of the Himalaya are, from west to east, Burang graben, the Thakkhola graben, Gyirong graben, Kungo graben, Pum Qu graben and Yadong graben. These grabens and associated other normal faults in the southern Tibet are characterized by the normal fault type earthquake with strike-slip component at approximate depth of 15 km.

North-East (NE) and North-West (NW) Nepal Source

A distinct cluster of seismic events is conspicuous in northwest and northeast Nepal. The cluster zone is connected with inferred strike-slip faults that connects the Shilong Plateau in the east (Diehl et al., 2017). Similarly, in the western Nepal, the events are mainly of strike-slip types associated with the Northwest fault. The events are clearly of strike-slip type with focal depth greater than 50 km, i.e. below the subduction interface (e.g. 2011 Taplejung-Sikkim earthquake) in the North-East source, however, for North-West source the focal depth is about15 km based on the instrumental earthquakes, which are considered accordingly in the model.

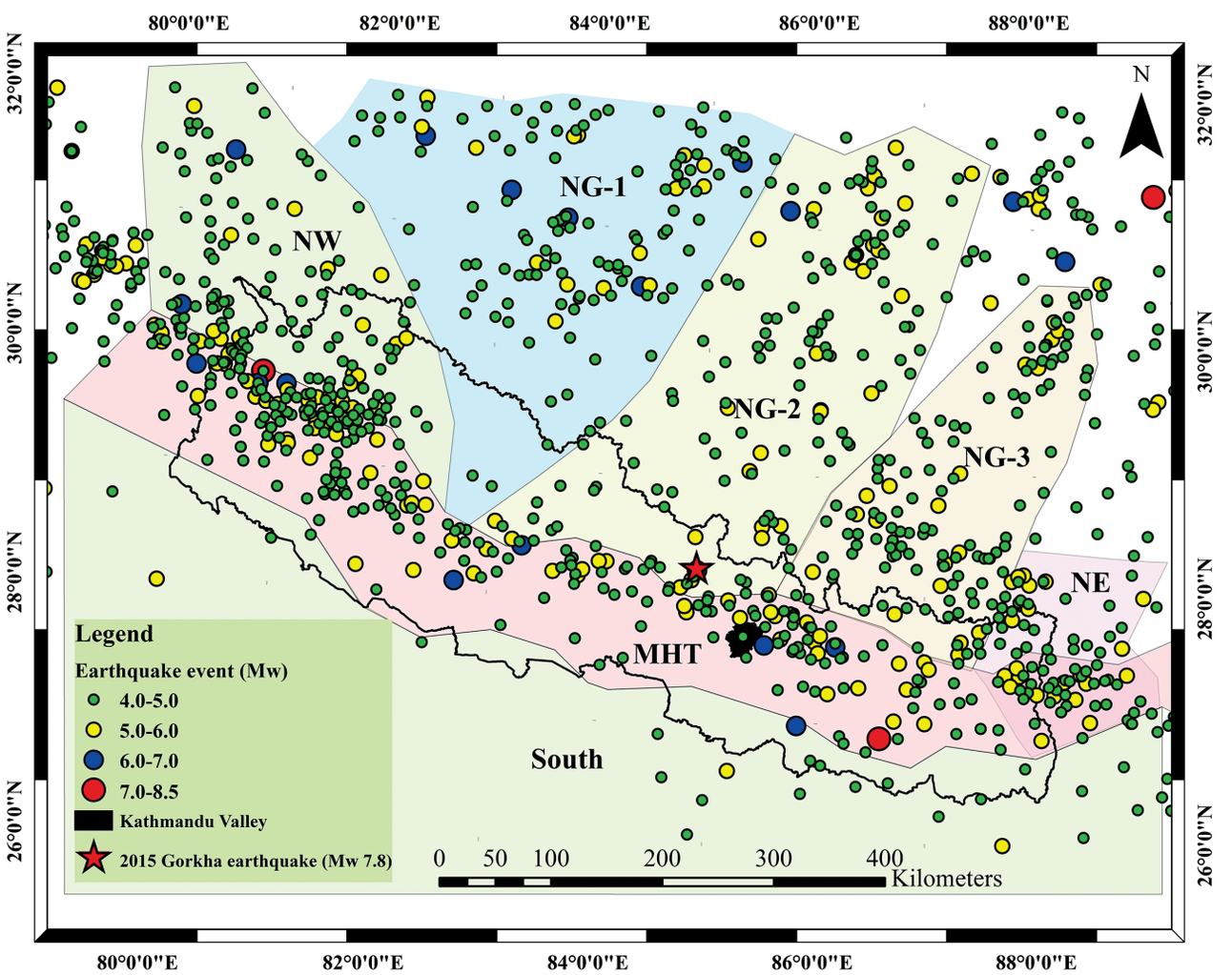

Fig. 5: Areal sources (except MHT) considered for the seismo-tectonic model. The source MHT is a fault source for which recurrence parameters are determined considering the events located in the locked portion shown by its periphery.

Southern Source

Unlikely, compare to the Himalayan belt, the seismic events are not frequent in the Indo-Gangetic plain. However, there are occasionally earthquakes of moderate magnitude, probably due to flexure of converging Indian plate. To incorporate the shaking of these earthquakes in the seismic model, the region is also considered as a separate seismic source with different seismogenic depths.

Completeness Test and Recurrence parameters

In order to get realistic earthquake recurrence parameters, completeness test of the catalogue is carried out for each seismic source. One of the techniques to test this completeness is to plot the rate of the earthquakes (number of events greater than a specified magnitude divided by the time period) as a function of time, starting at present time and moving back towards the beginning of the catalogue. If the rate of earthquakes is represented by a stationary Poisson process (the rate -λm- does not change with time) for the region, which is the typical assumption, then the rate of earthquakes should remain constant for the portions of the catalogue that have complete reporting. The completeness test of the catalogue was performed using the method developed by Stepp (1972), which includes generating completeness plots to visually inspect the rate of events over the years. The plots were developed starting at a minimum magnitude of 4.0 and carried out using varying sizes of magnitude bins.

The declustered catalogue was used for the characterization of the frequency of events (Fig. 2). The Gutenberg-Richter relationship, which is linear when the magnitude is plotted against the frequency of events on a semi-logarithmic scale, is used. The magnitude-frequency relation expressed in its cumulative form is:

$$\log N(M)=a-b*M$$

Where M is the magnitude and N is the cumulative frequency of earthquakes greater than magnitude M. For this study, a minimum magnitude of 4.0 was used to develop recurrence parameters. Recurrence parameters computed using the least square method is shown in Table 3 and Figure 6. The maximum magnitude for each source zone is based on the maximum magnitude earthquake occurred in each zone.

Ground Motion Prediction Equation

The Ground Motion Prediction Equation (GMPE) is one of the important parameters that govern the level of predicted ground motion at any site. Since there is no specific GMPE for the seismo-tectonics and seismicity of the Himalayan belt, several GMPEs are developed for different tectonic environments. However, in this study, GMPEs are selected on the basis of tectonic regimes. Tectonically, the MHT source is considered as a subduction interface between the converging plates, South, North grabens (NG-1, NG-2 and NG-3) are considered as the active shallow crusts and North-East and North-West sources are taken as the stable continental areas and relevant GMPEs are assigned accordingly (Fig. 5). The weight for each GMPE is assigned on their nature and personal judgement using logic-tree to incorporate contribution of Next Generation Attenuation (NGA) relations and other classical GMPEs (Fig. 7). It is believed that the adopted logic-tree approach reduces the uncertainty on computed hazard level.

Table 3: Seismicity Parameters for hazard estimation.

S. No	Sources	a	b	Minimum Magnitude (M_w)	Maximum Magnitude (M_w)	References for Maximum Magnitude (M_w)
1	MHT	4.10	0.78	4.00	8.40	Earthquake Catalogue
2	North East	4.68	1.04	4.00	6.90	Largest Recorded
3	North Graben-1	3.56	0.77	4.00	7.10	Elliot et al. (2010)
4	North Graben-2	3.86	0.82	4.00	7.10	Elliot et al. (2010)
5	North Graben-3	4.95	1.07	4.00	7.10	Elliot et al. (2010)
6	North West	4.18	0.88	4.00	7.10	Murphy et al. (2014)
7	South	4.36	1.01	4.00	7.00	Earthquake Catalogue

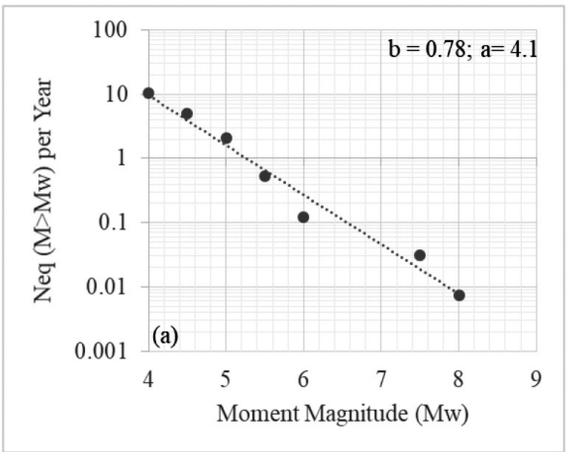

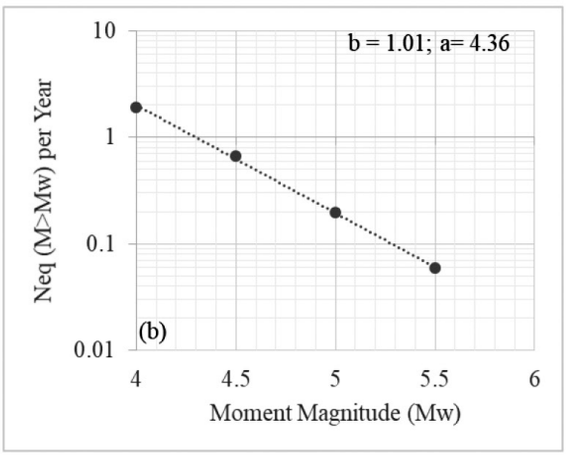

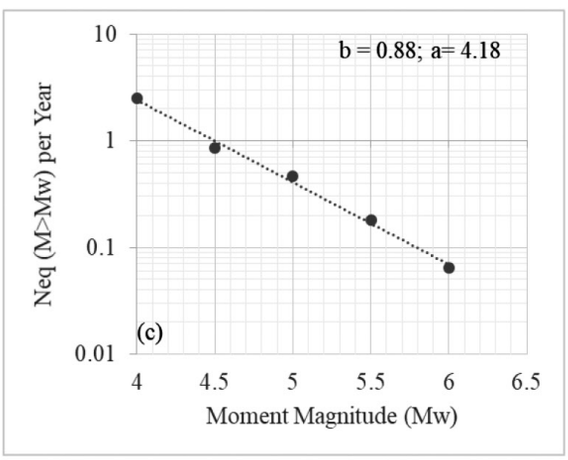

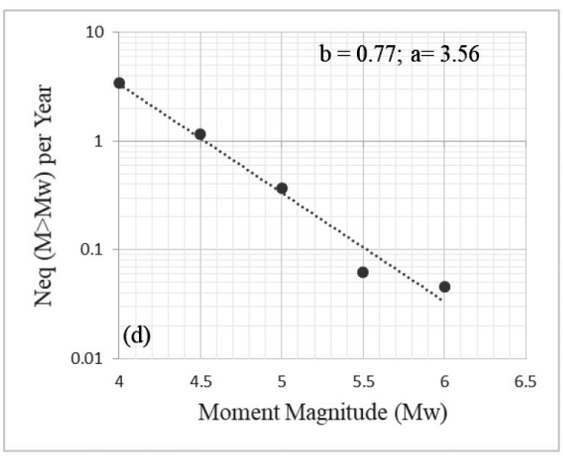

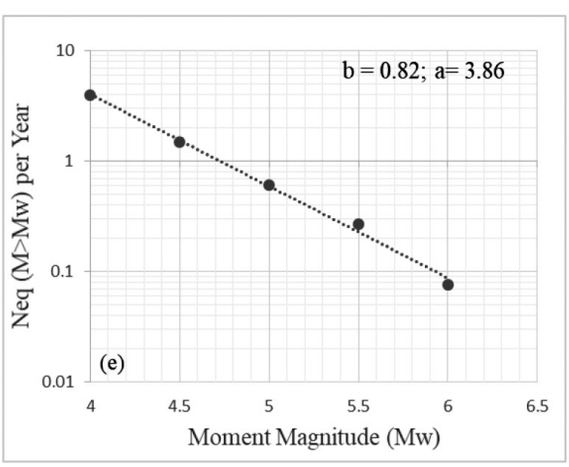

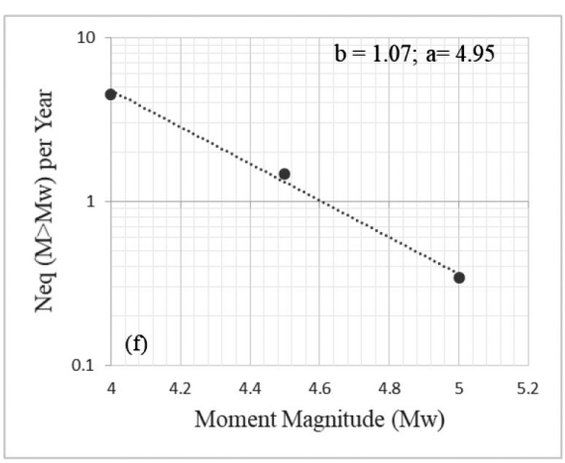

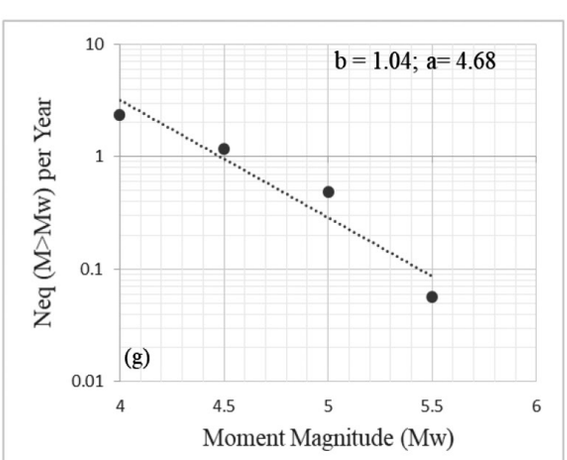

Fig. 6: The computed recurrence parameters for (a) Main Himalayan Thrust (b) South source (c) North West (d) North Graben-1 (e) North Graben-2 (f) North Graben-3 (g) North East.

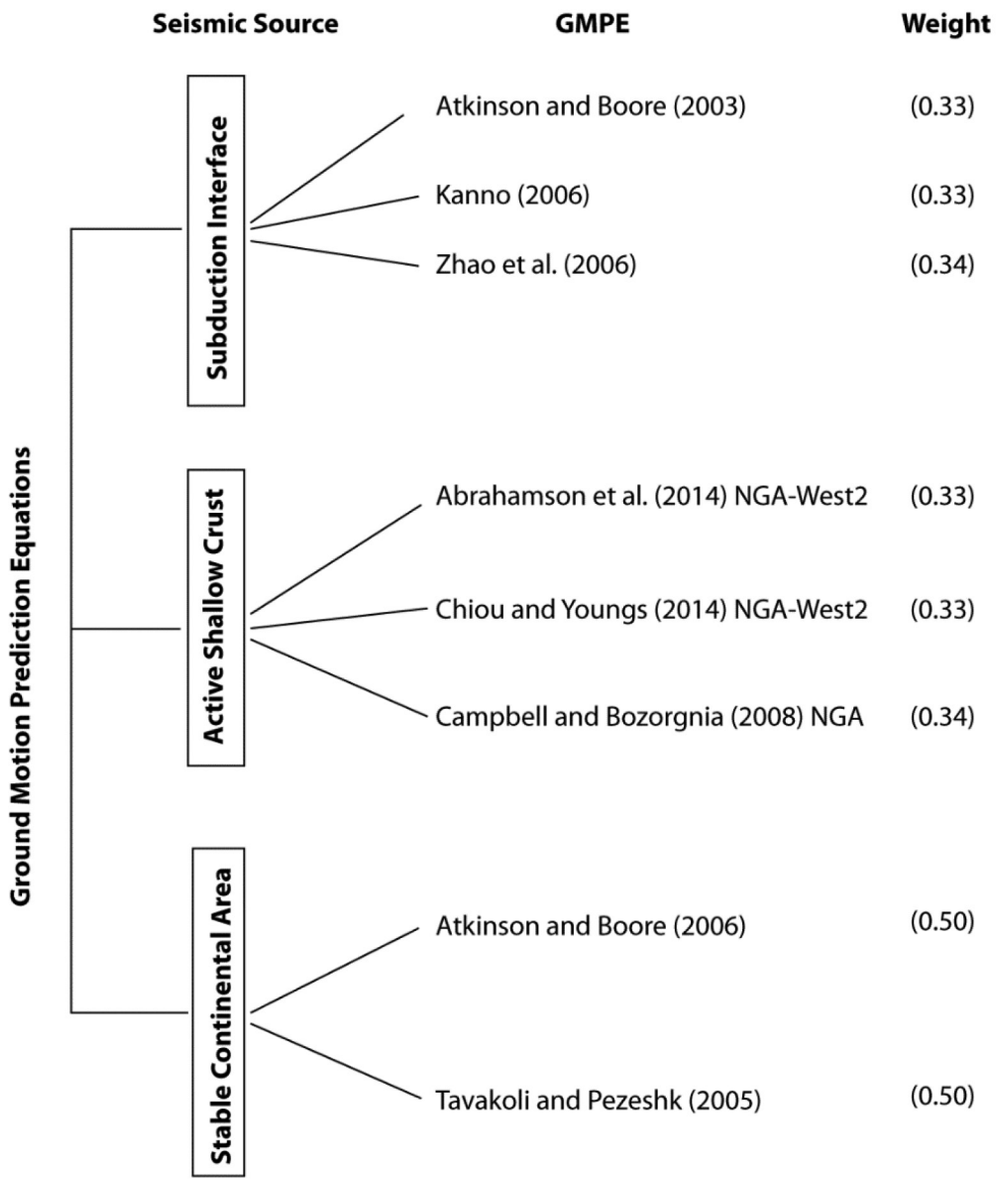

Fig. 7: Logic tree of GMPEs adopted for the computation of hazard.

Computational Code

Several codes are in use for seismic hazard computation and each code has its own characteristics, functionalities and limitations. Considering the nature of seismic sources (both aerial and fault source), the OpenQuake codes developed by Global Earthquake Model (GEM) (https://www.globalquakemodel.org/tools-products) are used. The codes provide many facilities to incorporate fault source, scenario earthquake, point source, aerial source, distributed seismicity and gridded seismicity sources etc. Since MHT is a complex subduction interface seismic source in the Himalayas, OpenQuake software can realistically incorporate complex fault geometry like flat-ramp-flat. Beside these, there are number of unique facilities in the code to assign probability for source parameters for hazard computation in user-friendly ways. To incorporate site effects in hazard level, an average shear wave velocity to a 30 m depth ($V_{s30)}$ is essential as demanded by each GMPEs considered in this study. The value of Vs30, 1140 m/s at bedrock level was used to compute the seismic hazard. This value was determined by Spatial Auto Correlation (SPAC) technique through an array measurement of ambient noise close to KTP station, Kirtipur.

RESULTS AND DISCUSSION

The site specific seismic hazard computation for Kirtipur (KTP) was performed for two different sources, e.g. (i) single ramp along the MHT

geometry with and without aerial sources, (ii) double ramp geometry along the MHT with and without aerial sources for 760 yr return period, which is approximately equivalent to return period of great earthquakes in Nepal. The results are then compared with the measured ground motion of mainshock of the 2015 Gorkha earthquake. In the single ramp model (SRM), a flat-ramp-flat geometry with single ramp is used, with and without areal sources. The PGA for source SRM along the MHT is 0.45 g, 0.25g and 0.19 g for return period of 2475 yr, 760 yr and 475 yr respectively (Table 4). Similar PGA values are obtained for seismic source SRM of the MHT and areal sources. In the second model, double ramp (DRM) with and without aerial sources are considered. For DRM along the MHT, slightly different results are obtained. For DRM along MHT source only, PGA values are 0.48 g, 0.27 g, 0.21g for return period of 2475 yr, 760 yr and 475 yr respectively (Table 4). The model with DRM and aerial sources has given same values of PGA like in the fault source only in all considered return periods. The obtained values for DRM model are slightly higher than the values obtained for SRM. Interestingly, incorporation of aerial sources with fault source did not give different results indicating that the areal sources have the least contribution. The computed PGA values for both SRM and DRM for 760 yr return period are comparable with measured PGA values at KTP rock site (Table 4 and Fig. 8). With this comparison, a seismic hazard assessment was carried out for the valley for 475 yr, 760 yr and 2475 yr return period. For return period of 760 yr, the PGA values vary from 0.24 g to 0.28 g in Kathmandu valley. The results show that the PGA values are gradually decreased towards north of the valley with the decrease in locking level of the MHT (Fig. 9). This pattern of PGA distribution is similar for other return periods (Figs. 10 and 11).

Table 4: Comparison of computed and measured PGAs.

Seismic Source	Peak ground acceleration (PGA) in g for return period of		
	475 yr	760 yr	2475 yr
Single Ramp Model (SRM)	0.19	0.25	0.45
Double Ramp Model (DRM)	0.21	0.27	0.48
SRM including all areal sources	0.19	0.25	0.45
DRM including all areal sources	0.21	0.27	0.48
Measured (SRSS) at KTP		0.26	

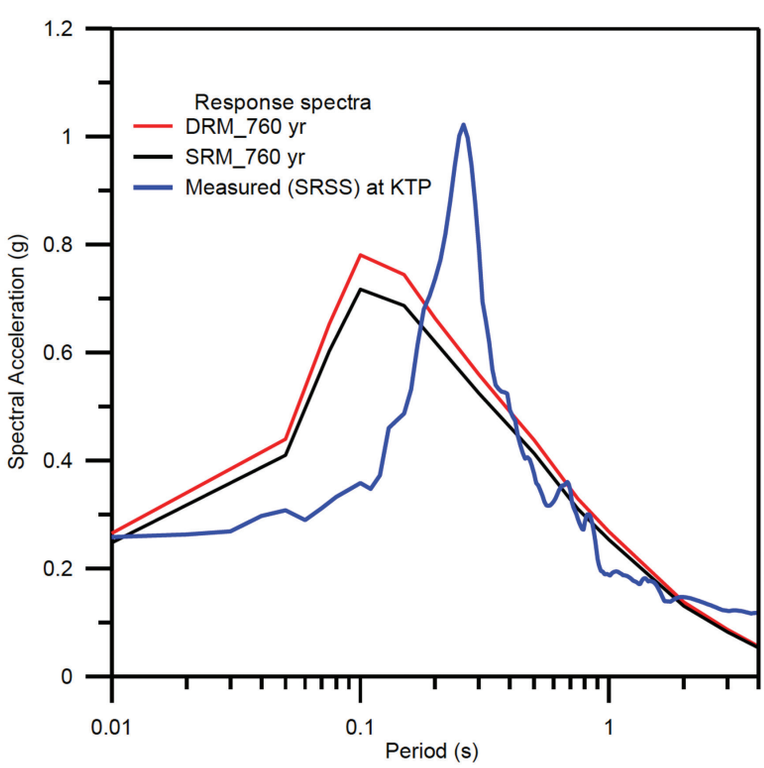

Fig. 8: Comparison of computed and measured response spectra at 5% damping. SRM: Single ramp model; DRM: Double ramp model.

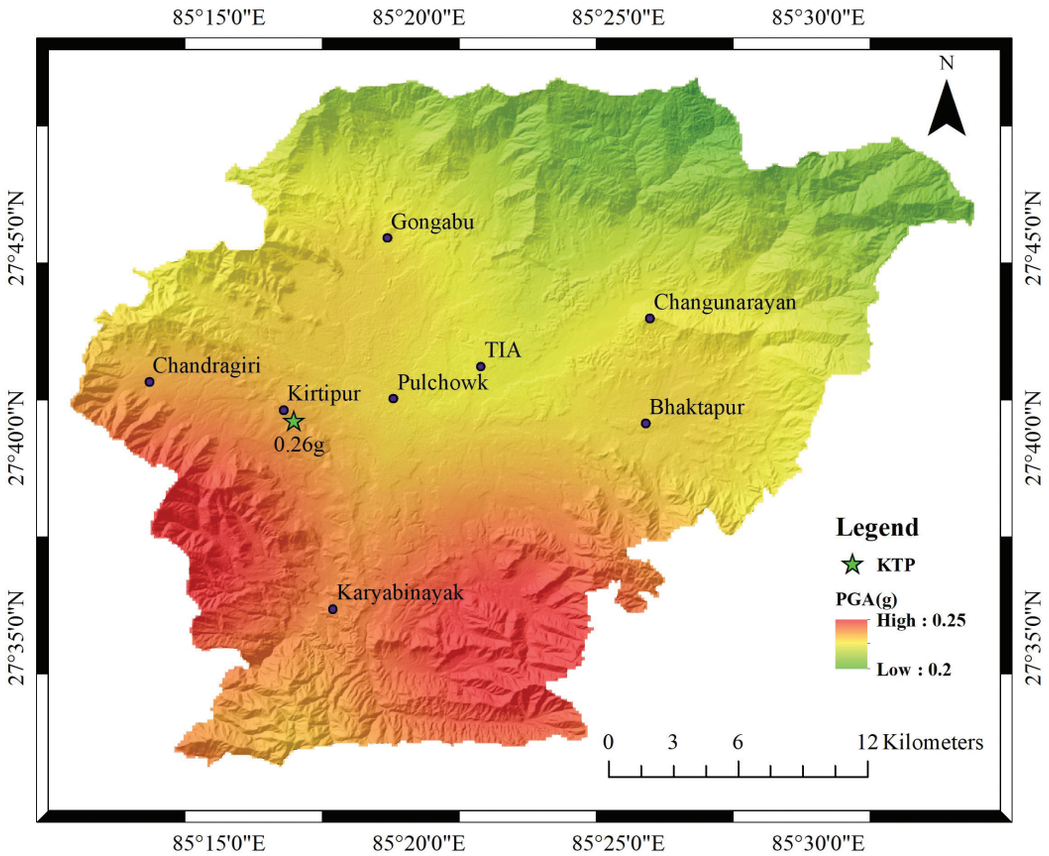

Fig. 9: Seismic hazard map for 760 yr return period for Kathmandu valley. Peak ground acceleration in g.

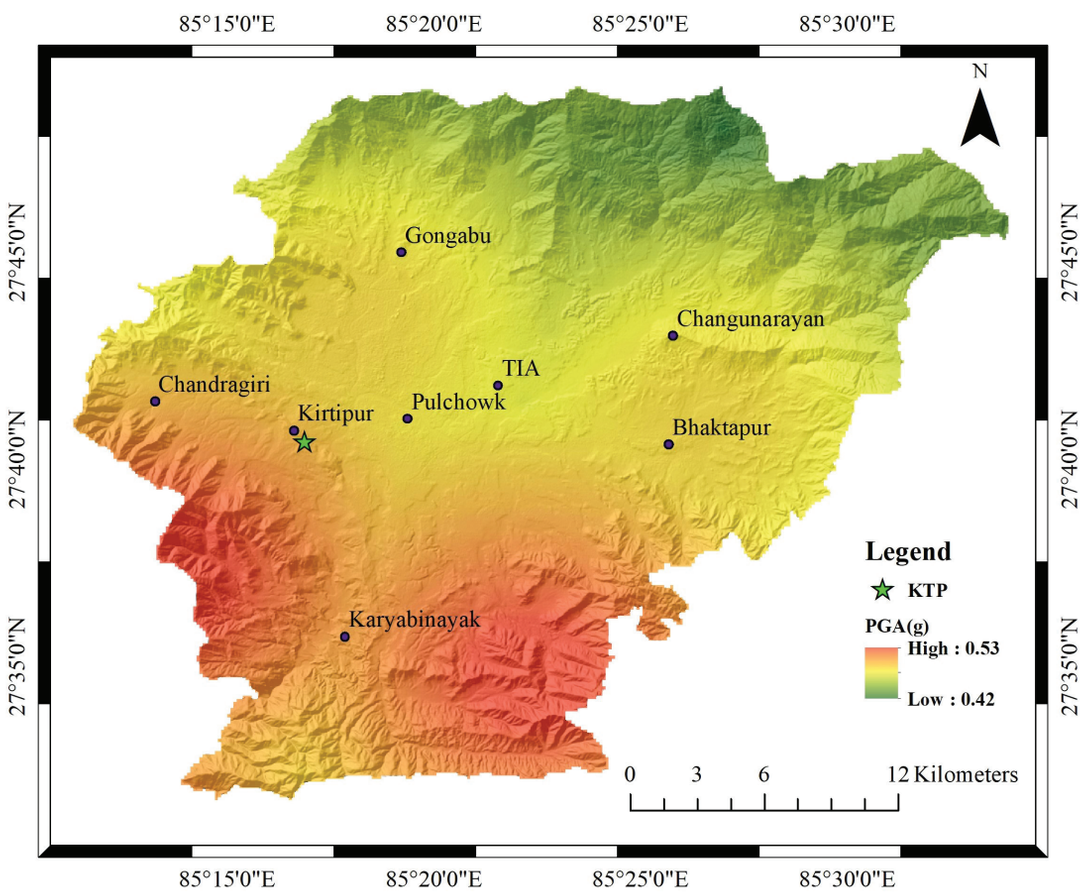

Fig. 10: Seismic hazard map for 2475 yr return period for Kathmandu valley. Peak ground acceleration in g.

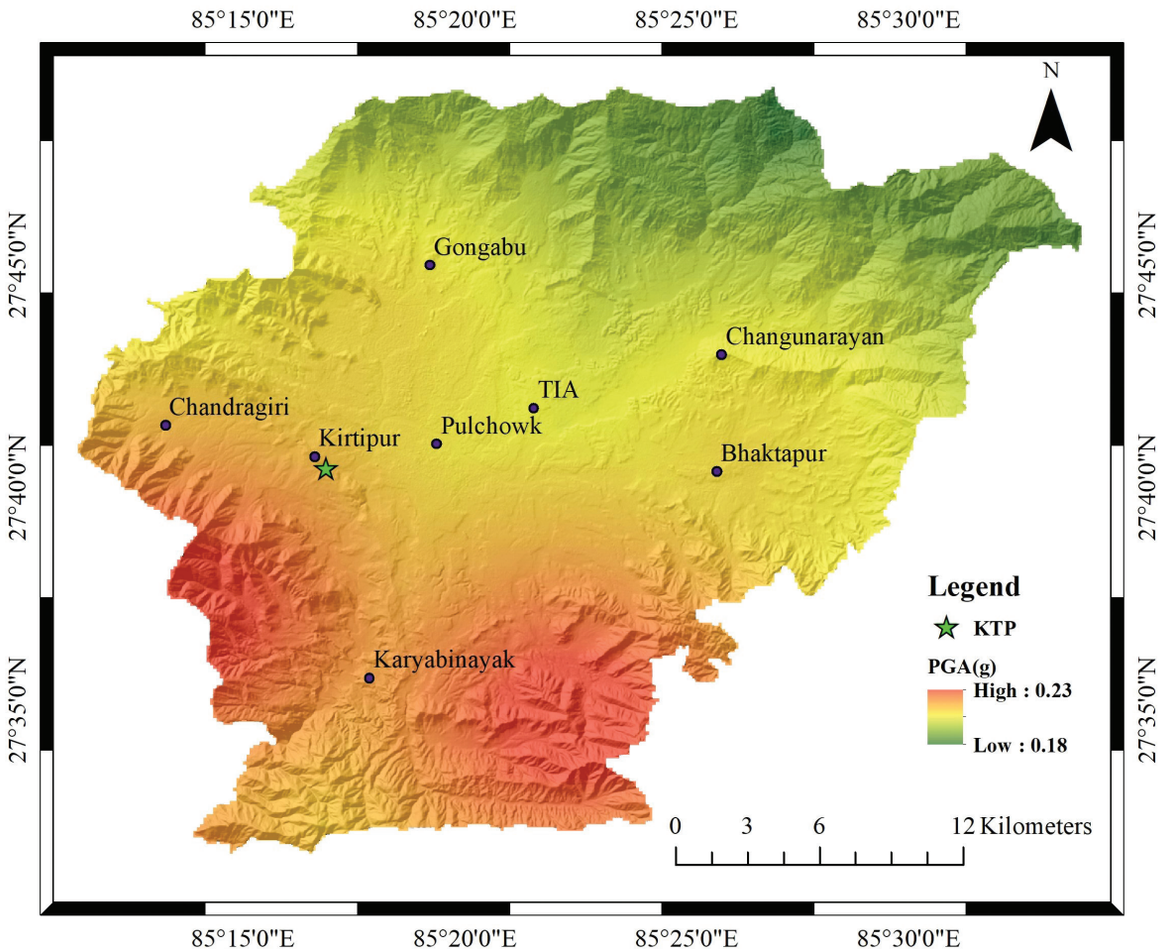

Fig. 11: Seismic hazard map for 475 yr return period for Kathmandu valley. Peak ground acceleration in g.

The disaggregation has also been carried out for Kirtipur site to understand the effects of most likely earthquakes. For Kirtipur, it can be seen that the most likely earthquakes to cause significant ground motion in Kathmandu valley are between magnitude 7 and 8.5 and distance up to roughly 60 km (Fig. 12). The hazard curves for SRM and SRM with aerial sources are same. Similar situation is also found for DRM and DRM with aerial sources (Fig. 13).

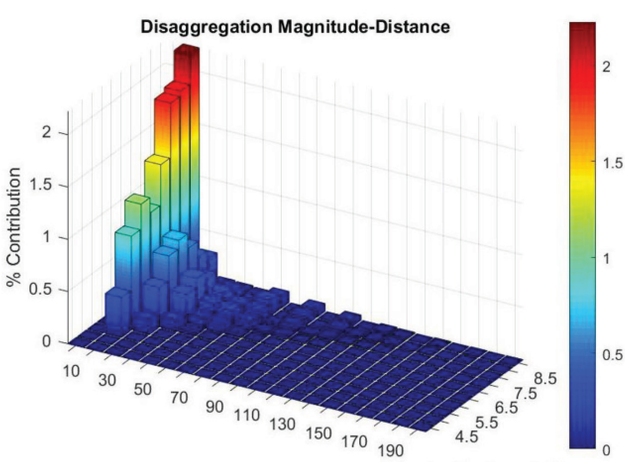

Fig. 12: Disaggregation for 760 yr return period for double ramp geometry of the MHT at Kirtipur, Kathmandu.

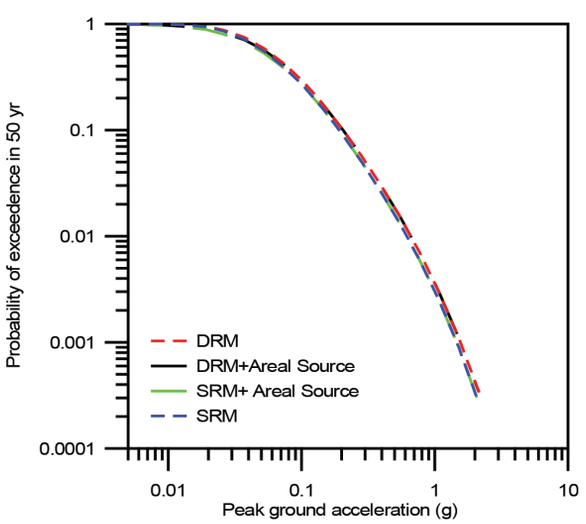

Fig. 13: Hazard curves for 760 yr return period for different seismic sources at Kirtipur, Kathmandu.

There are quite few studies on seismic hazard assessment in Nepal, particularly focussing Kathmandu valley, e.g. Pandey et al. (2002); Thapa and wang (2013), Stevens et al. (2018). Pandey et al. (2002) estimated roughly 0.2 g PGA value for 475 yr return period for Kathmandu at bed rock level using aerial and linear sources, which is quite less

than measured value for main shock of 2015 Gorkha earthquake. Thapa and Wang (2013) estimated PGA value in between 0.475 g to 0.525 g for return period of 475 yr. Recently, Stevens et al. (2018) computed seismic hazard for Nepal considering realistic aerial and seismogenic fault sources. Their estimation was quite higher (>0.5 g) for Kathmandu valley. The 2015 Gorkha earthquake occurred 760 year after the 1255 AD great earthquake that ruptured the MFT south of the 2015 Gorkha earthquake (Wesnousky et al., 2017a). The period of 760 year can be assumed as a probable return period for this segment of MFT based on paleoseimc investigations in central and eastern Nepal (e.g. Sapkota et al., 2013; Bollinger et al., 2014). In the present study, both fault and aerial sources are considered and efforts have been made to get realistic comparison with the measured values. The geometrical complexities of the MHT has been carefully addressed to understand its relative contribution in seismic hazard in Kathmandu valley. The computed PGA values are similar for both sources, i.e. SRM or DRM with and without aerial sources, means that the aerial sources do not have significant contribution for seismic hazard in Kathmandu valley. In case of fault source only, i.e. MHT, the effect of complex geometry has been seen on hazard level. The computed PGA values, i.e. 0.27 g and 0.25 g for return period of 760 yr with DRM and SRM excluding aerial sources, are roughly consistent with the square root of sum of square (SRSS) of the measured horizontal PGA (0.26 g) at KTP site. The difference of ±3.84% is attributed to selection of GMPEs and may be significantly reduced by developing realistic GMPE for the Himalayan region. Thus, it is found that the contribution of complex geometry of the MHT is not significant in case of quantitative estimation as mentioned by Chamlagain et al. (2019). Based on the findings of recent studies in central Nepal, however, the hazard analysis adopting DRM along the MHT is proposed as a preferable estimation.

CONCLUSIONS

Kathmandu valley, a major intermontane basin, in central Nepal is located just above the seismogenic thrust fault called the Main Himalayan Thrust (MHT). There are mainly two geometries of the MHT; first a single deeper ramp at the mid-crustal level and, secondly moderate ramp below the Mahabharat range and deeper ramp at mid-crustal level. The contribution of these geometries and areal source on seismic hazard in Kathmandu valley has been investigated adopting measured shear wave velocity at 30 m depth and different ground motion prediction equations developed for the specific tectonic environment. The obtained results have shown less contribution of aerial sources in hazard as the valley is located above the thrust that usually ruptures during the devastating earthquake in the region. There is no significant difference on hazard level considering single and double ramp fault geometries separately**.** The single and double ramp geometries gave peak ground acceleration of 0.25 g and 0.27 g respectively for 760 yr return period. These values are very close to measured acceleration, i.e. 0.26 g of the 2015 Gorkha earthquake that occurred 760 years after the 1255 AD great earthquake. The difference is about ±3.84% and may be attributed to lack of relevant ground motion prediction equation for the Himalaya. The obtained spatial hazard pattern is consistent with the locking nature of the Main Himalayan Thrust, i.e. locking is relatively waning out towards north. It is understood that considering seismogenic fault as an earthquake source provide better results consistent with the ongoing neotectonic deformation in central Nepal. The study, therefore, concludes that the geometry of the MHT should precisely be characterised while carrying out the seismic hazard assessment in the Himalaya.

AUTHOR'S CONTRIBUTIONS

The research was conceptualized by D. Chamlagain. The seismo-tectonic model was prepared by D. Chamlagain and both authors discussed and finalized. Computation of seismic hazard was carried out by G.P. Niroula under the supervision of D. Chamlagain. The manuscript was drafted by D. Chamlagain and both authors read, discussed and approved the manuscript.

REFERENCES

Abrahamson, N. A., Silva, W. J., & Kamai, R., 2014, Summary of the ASK14 ground motion relation for active crustal regions. Earthquake Spectra, v. 30(3), pp. 1025–1055.

Ader,T. A., 2012, Convergence rate across the Nepal Himalaya and Interseismic Coupling on the Main Himalayan Thrust: implications for seismic hazard. Journal of Geophysical Research, v. 117(B4), p.B04403.

Atkinson, G.M. and Boore, D.M., 2006, Earthquake ground-motion prediction equations for eastern North America, Bulletin of the Seismological Society of America, v.96, pp. 2181-2205.

Atkinson, G.M., and Boore, D.M, 2003, Empirical ground-motion relations for subduction zone earthquakes and their application to Cascadia and other regions. Bulletin of the Seismological Society of America, v. 93(4), pp.1703–1729.

Avouac, J.P., Meng, L., Wei, S., Wang, T. and Ampuero, J.P., 2015, Lower edge of locked Main Himalayan Thrust unzipped by the 2015 Gorkha earthquake. Nature Geoscience, v. 8(9), pp.708-711.

Bollinger, L., Sapkota, S.N., Tapponnier, P., Klinger, Y., Rizza, M., Van Der Woerd, J., Tiwari, D.R., Pandey, R., Bitri, A. and Bes de Berc, S., 2014, Estimating the return times of great Himalayan earthquakes in eastern Nepal: Evidence from the Patu and Bardibas strands of the Main Frontal Thrust. Journal of Geophysical Research: Solid Earth, v. 119(9), pp.7123-7163.

Campbell, K.W., Bozorgnia, Y., 2008, NGA ground motion model for the geometric mean horizontal component of PGA, PGV, PGD and 5 % damped linear elastic response spectra for periods ranging from 0.01 to 10 s. Earthquake Spectra, v. 24(1), pp.139–171.

Chamlagain, D., Anderson, J.G. and Wesnousky, S.G. 2019, Epistemic uncertainty on probabilistic seismic hazard considering the Main Himalayan Thrust (MHT) in Nepal Himalaya. Proceedings on International Conference on Disaster Risk Management, Dhaka, Bangladesh, January 12-14, 2019.

Chiou, B. S. J., and Youngs, R. R., 2014, Update of the Chiou and Youngs NGA model for the average horizontal component of peak ground motion and response spectra. Earthquake Spectra, v. 30(3), pp.1117–1153.

Cornell, C.A., 1968, Engineering seismic risk analysis. Bulletin of the Seismological Society of America, v. 58(5), pp.1583-1606.

DeCelles, P.G., Robinson, D.M., Quade, J., Ojha, T.P., Garzione, C.N., Copeland, P. and Upreti, B.N., 2001, Stratigraphy, structure, and tectonic evolution of the Himalayan fold-thrust belt in western Nepal. Tectonics, v. 20(4), pp.487-509.

Dhakal, Y.P., Kubo, H., Suzuki, W. et al., 2016, Analysis of strong ground motions and site effects at Kantipath, Kathmandu, from 2015 Mw 7.8 Gorkha, Nepal, earthquake and its aftershocks. Earth Planets Space v. 68, pp. 1-12 https://doi.org/10.1186/s40623-016-0432-2

Diehl, T., Singer, J., Hetényi, G., Grujic, D., Clinton, J., Giardini, D., Kissling, E. and GANSSER Working Group, 2017, Seismotectonics of Bhutan: Evidence for segmentation of the Eastern Himalayas and link to foreland deformation. Earth and Planetary Science Letters, v. 471, pp. 54-64.

Elliott, J.R., Jolivet, R., González, P.J., Avouac, J.P., Hollingsworth, J., Searle, M.P. and Stevens, V.L., 2016, Himalayan megathrust geometry and relation to topography revealed by the Gorkha earthquake. Nature Geoscience, v. 9(2), pp.174-180.

Elliott, J.R., Walters, R.J., England, P.C., Jackson, J.A., Li, Z. and Parsons, B., 2010, Extension on the Tibetan plateau: recent normal faulting measured by InSAR and body wave seismology. Geophysical Journal International, v. 183(2), pp.503-535.

Gardner, J.K. and Knopoff, L., 1974, Is the sequence of earthquakes in Southern California, with aftershocks removed, Poissonian? Bulletin of the Seismological Society of America, v. 64(5), pp.1363-1367.

Hubbard, J., Almeida, R., Foster, A., Sapkota, S.N., Bürgi, P. and Tapponnier, P., 2016, Structural segmentation controlled the 2015 Mw 7.8 Gorkha earthquake rupture in Nepal. Geology, v. 44(8), pp.639-642.

Kanno, T., Narita, A., Morikawa, N., Fujiwara, H., and Fukushima, Y., 2006, A new attenuation relation for strong ground motion in Japan based on recorded data. Bulletin of the Seismological Society of America, 96(3): pp. 879–897.

Katel, T.P., Upreti, B.N. and Pokharel, G.S., 1996, Engineering properties of fine grained soils of the Kathmandu Valley, Nepal. Journal of Nepal Geological Society 13:128-138

Kubo, H., Dhakal, Y.P., Suzuki, W., Kunugi, T., Aoi, S. and Fujiwara, H., 2016, Estimation of the source process of the 2015 Gorkha, Nepal, earthquake and simulation of long-period ground motions in the Kathmandu basin using a one-dimensional basin structure model. Earth, Planets and Space, v. 68(1), p.16.

Lavé, J., Yule, D., Sapkota, S., Basant, K., Madden, C., Attal, M. and Pandey, R., 2005, Evidence for a great Medieval earthquake (~ 1100 AD) in the central Himalayas, Nepal. Science, v. 307(5713), pp.1302-1305.

Le Fort, P., 1975, Himalayas: the collided range. Present knowledge of the continental arc. American Journal of Science, v. 275(1), pp.1-44.

Lemonnier, C., Marquis, G., Perrier, F., Avouac, J.P., Chitrakar, G., Kafle, B., Sapkota, S., Gautam, U., Tiwari, D. and Bano, M., 1999, Electrical structure of the Himalaya of central Nepal: High conductivity around the mid-crustal ramp along the MHT. Geophysical Research Letters, v. 26(21), pp.3261-3264.

Ministry of Home Affairs, 2016, Gorkha earthquake-2015: Experience and Learning. Ministry of Home Affairs, 250p.

Moribayashi, S., 1980, Basement topography of the Kathmandu Valley, Nepal: an application of gravitational method to the survey of a tectonic basin in the Himalayas. Journal of The Japan Society of Engineering Geologist, v. 21, pp.30-37.

Mugnier, J.L., Gajurel, A., Huyghe, P., Jayangondaperumal, R., Jouanne, F. and Upreti, B., 2013, Structural interpretation of the great earthquakes of the last millennium in the central Himalaya. Earth-Science Reviews, v. 127, pp.30-47.

Murphy, M. A., Taylor, M. H. T., Gosse, J., Silver, C. R. P., Whipp, D. M., and Beaumont, C., 2014, Limit of strain partitioning in the Himalaya marked by large earthquakes in western Nepal, Nature Geoscience, v. **7**, pp. 38– 42.

Pandey, M.R., Chitrakar, G.R., Kafle, B., Sapkota, S.N., Rajaure, S.N. and Gautam, U.P., 2002, Seismic hazard map of Nepal. Kathmandu: Department of Mines and Geology.

Pandey, M.R., Tandukar, R.P., Avouac, J.P., Lave, J. and Massot, J.P., 1995, Interseismic strain accumulation on the Himalayan crustal ramp (Nepal). Geophysical Research Letters, v. 22(7), pp.751-754.

Pandey, M.R., Tandukar, R.P., Avouac, J.P., Vergne, J. and Heritier, T., 1999, Seismotectonics of the Nepal Himalaya from a local seismic network. Journal of Asian Earth Sciences, v. 17(5-6), pp.703-712.

Pant, M. R., 2002, A step towards a historical seismicity of Nepal. Adarsa, 29–60, Kathmandu: Pundit Publication

Rahman, M.M., Bai, L., Khan, N.G. and Li, G., 2018, Probabilistic seismic hazard assessment for Himalayan–tibetan region from historical and instrumental earthquake catalogs. In Earthquakes and Multi-hazards Around the Pacific Rim, V. II (pp. 161-181). Birkhäuser, Cham.

Rana B.J.B., 1935, *Nepal ko Maha Bhukampa (Great earthquake of Nepal).* Kathmandu: Jorganesh Press.

Sakai H., 2001, Stratigraphic division and sedimentary facies of the Kathmandu Basin Group, central Nepal. Journal of Nepal Geological Society 25(Sp. Issue), pp. 19-32.

Sapkota, S.N., Bollinger, L., Klinger, Y., Tapponnier, P., Gaudemer, Y. and Tiwari, D., 2013, Primary surface ruptures of the great Himalayan earthquakes in 1934 and 1255. Nature Geoscience, v. 6(1), pp.71-76.

Schelling, D. and Arita, K., 1991, Thrust tectonics, crustal shortening, and the structure of the far-eastern Nepal Himalaya. Tectonics, v. 10(5), pp.851-862.

Schnabel, P.B. 1973, Effects of Local Geology and Distance from Source on Earthquake Ground Motion, Ph.D. Thesis, University of California, Berkeley, California

Scordilis, E.M., 2006, Empirical global relations converting ms and mb to moment magnitude. Journal of Seismology, v. 10(2), pp.225-236.

Stepp, J.C., 1972, Analysis of completeness of the earthquake sample in the Puget Sound area and its effect on statistical estimates of earthquake hazard. In Proc. of the 1st Int. Conf. on Microzonazion, Seattle, v. 2, pp. 897-910.

Stevens, V.L. and Avouac, J.P., 2016, Millenary Mw> 9.0 earthquakes required by geodetic strain in the Himalaya. Geophysical Research Letters, v. 43(3), pp.1118-1123.

Stevens, V.L., Shrestha, S.N. and Maharjan, D.K., 2018, Probabilistic Seismic Hazard Assessment of Nepal. Bulletin of the Seismological Society of America, v. 108(6), pp.3488-3510.

Stöcklin, J. and Bhattarai, K.D., 1977, Geology of Kathmandu area and central Mahabharat Range, Nepal Himalaya. HMG/UNDP mineral exploration project. Technical report, 86 p (with 15 maps), unpublished.

Takai, N., Shigefuji, M., Rajaure, S., Bijukchhen, S., Ichiyanagi, M., Dhital, M.R. and Sasatani, T., 2016, Strong ground motion in the Kathmandu Valley during the 2015 Gorkha, Nepal, earthquake. Earth, Planets and Space, v. 68(1), pp.1-8.

Tavakoli, B., and Pezeshk, S., 2005, Empirical-stochastic ground-motion prediction for eastern North America, Bulletin of the Seismological Society of America, v. 95, pp. 2283–2296.

Thapa, D.R., and Wang, G., 2013, Probabilistic seismic hazard analysis in Nepal. Earthquake Engineering and Engineering Vibration, v. 12(4), pp. 577-586.

Vucetic, M. and Dobry, R. 1991, Effect of Soil Plasticity on Cyclic Response. Journal of Geotechnical Engineering, v. 117, pp. 89-107.

Wang, X., Wei, S. and Wu, W., 2017, Double-ramp on the Main Himalayan Thrust revealed by broadband waveform modeling of the 2015 Gorkha earthquake sequence. Earth and Planetary Science Letters, v. 473, pp. 83-93.

Wesnousky, S.G., Kumahara, Y., Chamlagain, D., Pierce, I.K., Karki, A. and Gautam, D., 2017a, Geological observations on large earthquakes along the Himalayan frontal fault near Kathmandu, Nepal. Earth and Planetary Science Letters, v. 457, pp. 366-375.

Wesnousky, S.G., Kumahara, Y., Chamlagain, D., Pierce, I.K., Reedy, T., Angster, S.J. and Giri, B., 2017b, Large paleoearthquake timing and displacement near Damak in eastern Nepal on the Himalayan Frontal Thrust. Geophysical Research Letters, v. 44(16), pp. 8219-8226.

Zhao, J. X., Zhang, J., Asano, A., Ohno, Y., Oouchi, T., Takahashi, T., 2006, Attenuation relations of strong ground motion in Japan using site classification based on predominant period. Bulletin of the Seismological Society of America, 96(3), pp. 898–913.